REPRINT

EUROPTO® SERIES

Reprinted from

Sensors, Systems, and Next-Generation Satellites III

20–23 September 1999
Florence, Italy

Volume 3870

Development of ADEOS-II/GLI operational algorithm for earth observation

Teruyuki NAKAJIMA[1], Takashi Y. NAKAJIMA[2], Masakatsu NAKAJIMA[3]
and the GLI Algorithm Integration Team (GAIT)[2]

[1] Center for Climate System Research, The University of Tokyo, 4-6-1 Komaba, Meguro-ku, Tokyo 153-8904, Japan
[2] EORC / National Space Development Agency of Japan
[3] EOS / National Space Development Agency of Japan

ABSTRACT

GLI (Global Imager) is a 36 channel visible and infrared radiometer/imager onboard the NASDA/ADEOS-II satellite. The information carried by GLI for the earth-atmosphere system is huge and difficult to be extracted enough efficiently with an operational satellite data analyzing system. We discuss and overview the algorithm development of the GLI Level-2 products at NASDA/EORC. We have several innovations to make the system unique and efficient. GLI simulator and GLI synthetic data sets are among those, which will be useful even for the science and engineering communities of other earth observation satellite systems. We will also overview the current status of the entire GLI project.

Key words: Satellite, Imager, Visible and infrared radiometer, Earth Observation

1. INTRODUCTION

The Global Imager (GLI) is a 36 channel visible/infrared cross tracking imaging radiometer on board the ADEOS-II satellite (Advanced Earth Observing Satellite-II) scheduled to be launched in November 2000. The project of GLI has been developed for monitoring the earth's surface and lower atmosphere in order to contribute to several important sciences such as studies of global warming phenomenon, global water and energy circulation, and carbon cycle. For this purpose, the hardware has been designed so as to have optimum channel specifications and tilting mirror mechanism to enhance the coverage of monitoring.

After the last report (T. Nakajima et al., 1997)[1], there has been significant progress in the GLI project for the hardware and software developments. In this report those progresses are overviewed.

2. HARDWARE DEVELOPMENT

Table 1 show the channel specifications of GLI. The GLI has ocean color channels of improved sensitivity and other channels for general applications with large dynamic range. Those channel specifications have been designed with detailed calculation of radiative transfer (T. Y. Nakajima et al., 1998)[2] . It has a tilting scan mechanism similar to ADEOS/OCTS to avoid the sun glitter for ocean color remote sensing. There

For further author information -
T. Nakajima: 4-6-1 Komaba, Meguro-ku, Tokyo 153-8904, Japan, TEL. +81-3-5453-3959, FAX. +81-3-5453-3964, e-mail. teruyuki@ccsr.u-tokyo.ac.jp, home page. http://www. ccsr.u-tokyo.ac.jp/
T. Y. Nakajima: 1-9-9, Roppongi, Minato-ku, Tokyo 106-0032, TEL +81-3-3224-7089, FAX +81-3-3224-7051, e-mail. nakajima@eorc.nasda.go.jp, home page. http://www.eorc.nasda.go.jp/
M. Nakajima: 2-4-1, Hamamatsu-cho, Minato-ku, Tokyo 105-8060, TEL +81-3438-6367; FAX +81-3-5401-8702, e-mail. nakajima@rd.tksc.nasda.go.jp, home page: http://www.nasda.go.jp/

Part of the EUROPTO Conference on Sensors, Systems, and Next-Generation Satellites V
Florence, Italy • September 1999 SPIE Vol. 3870 • 0277-786X/99/$10.00

Table 1 GLI Channel Specifications. Channel number n, center wavelength WL (micron), half height full width DWL (micron) , nadir view resolution DST (km), standard radiance LST (W/m2/str/micron), inflection point of the piecewise linear amplifier LPS (W/m2/str/micron), maximum radiance LMX (W/m2/str/micron), signal to noise ratio SN, standard temperature TST (K), low standard temperature TLW (K), NEDT at the standard temperature NEDT, NEDT at the low standard temperature NEDTL, resolution of AD-comverter AMP (p with piecewise linear amplifier), and application OLAC (O: Ocean, L: Land, A: Atmosphere, C: Cryosphere).

n	WL	DWL	DST	LST	LPW	LMX	SN	AMP	OLAC	Comment
1	0.380	0.01	1	59		365	770	12	x-xx	DOM
2	0.400	0.01	1	70		139	1272	12	x---	baseline, DOM
3	0.412	0.01	1	65		130	1302	12	x---	chl-a, DOM
4	0.443	0.01	1	54	109	560	918	12P	xxx-	chl-a max
5	0.460	0.01	1	54	108	624	886	12P	xxx-	ocean pigment
6	0.490	0.01	1	43		86	1354	12	x---	ocean pigment
7	0.520	0.01	1	31	64	539	670	12P	x---	SS, high conc. ocean pigment
8	0.545	0.01	1	28	56	549	609	12P	x-xx	no ocean pigment
9	0.565	0.01	1	23		47	1128	12	xx--	min. pigment abs.
10	0.625	0.01	1	17		33	1026	12	x---	min. pigment
11	0.666	0.01	1	13		26	909	12	x---	baseline of fluor., atmos. corr.
12	0.680	0.01	1	12		24	911	12	xxx-	fluorescence
13	0.678	0.01	1	12		438	238	12	-xxx	chl-a abs
14	0.710	0.01	1	10		18	838	12	x---	baseline of fluor.
15	0.710	0.01	1	10		311	273	12	-xxx	
16	0.749	0.01	1	7		14	700	12	x---	atmos. corr.
17	0.763	0.008	1	6		350	148	12	-xx-	oxygen abs., liquid water content
18	0.865	0.02	1	5		9	552	12	x---	atmos. corr.
19	0.865	0.01	1	5		304	124	12	-xxx	cloud opt. thik., aerosols
20	0.460	0.07	0.25	36		624	206	12	-x--	vegetation
21	0.545	0.05	0.25	25		549	154	12	-xxx	vegetation, activities
22	0.660	0.06	0.25	14		150	179	12	-x--	vegetation, chl-a abs.
23	0.825	0.11	0.25	21		257	314	12	-xxx	vegetation, biomass
24	1.050	0.02	1	8		203	312	12	-xxx	water/ice/snow
25	1.13	0.07	1	8		167	369	12	--x-	water vapor abs.
26	1.240	0.02	1	5.4		138	303	12	-xxx	water/ice/snow
27	1.380	0.04	1	1.5		94	132	12	--x-	water vapor abs., cirrus
28	1.640	0.20	0.25	5		69	227	12	-xxx	vegetation, soil moisture, ice phase
29	2.210	0.22	0.25	1.3		30	86	12	-xxx	cloud droplet size, soil moisture

n	WL	DWL	DST	TST	TLW	NEDT	NEDTL	AMP		
30	3.715	0.33	1	300	250	0.15	1.8	12	x-xx	cloud phase
31	6.700	0.5	1	300	200	0.08	1.5	12	--x-	water vapor
32	7.300	0.5	1	300	200	0.07	1.0	12	--x-	water vapor
33	7.500	0.5	1	300	200	0.09	1.0	12	--x-	water vapor
34	8.600	0.5	1	300	180	0.08	0.5	12	x-xx	water vapor, ice/snow temp.
35	10.800	1.0	1	300	180	0.09	0.5	12	x-xx	SST, ice/snow temp., cloud top temp.
36	12.000	1.0	1	300	180	0.09	0.5	12	x-xx	SST, ice/snow temp., cloud top temp.

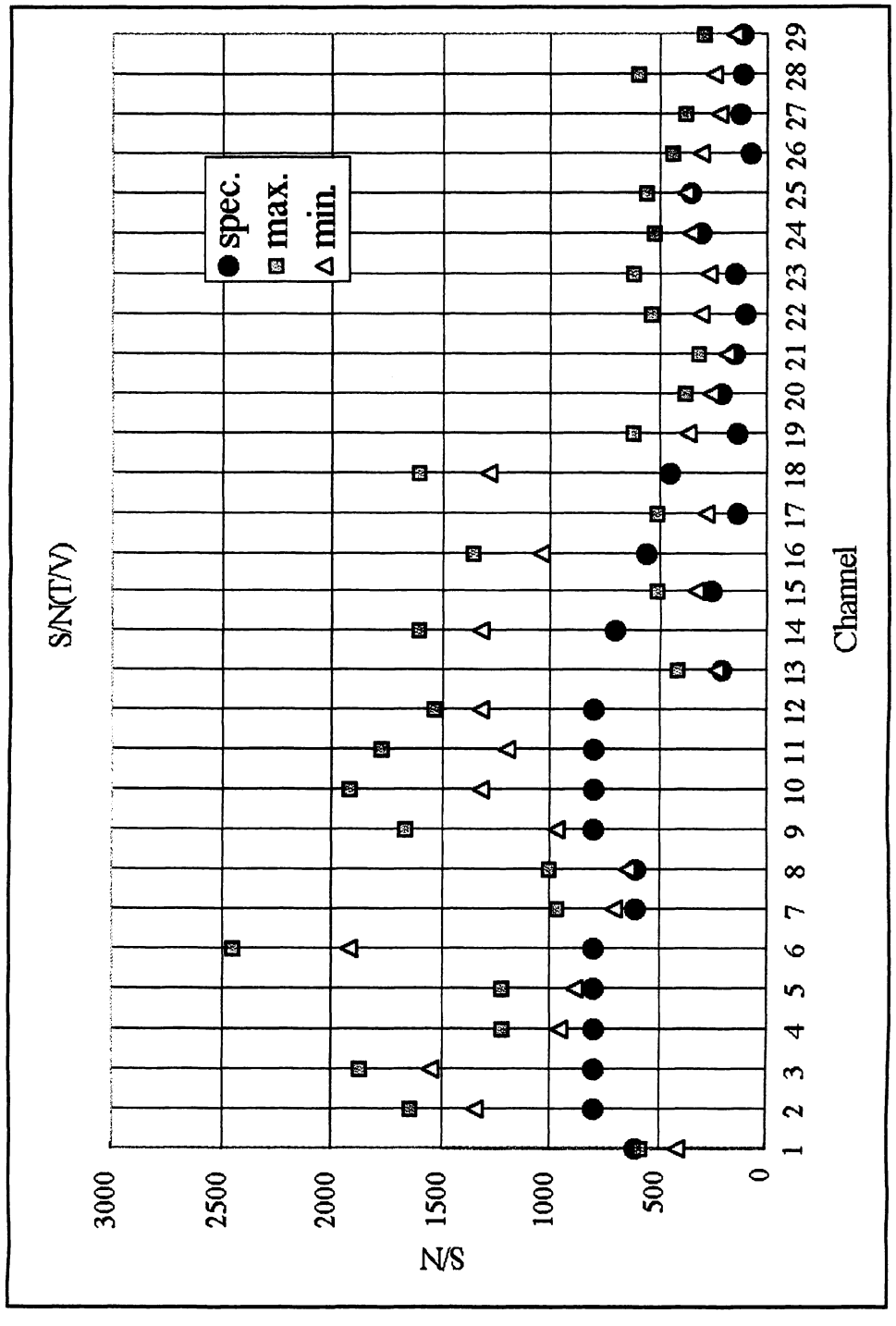

Figure 1 S/N ratio of the GLI channels (Ch.1 - Ch. 29)

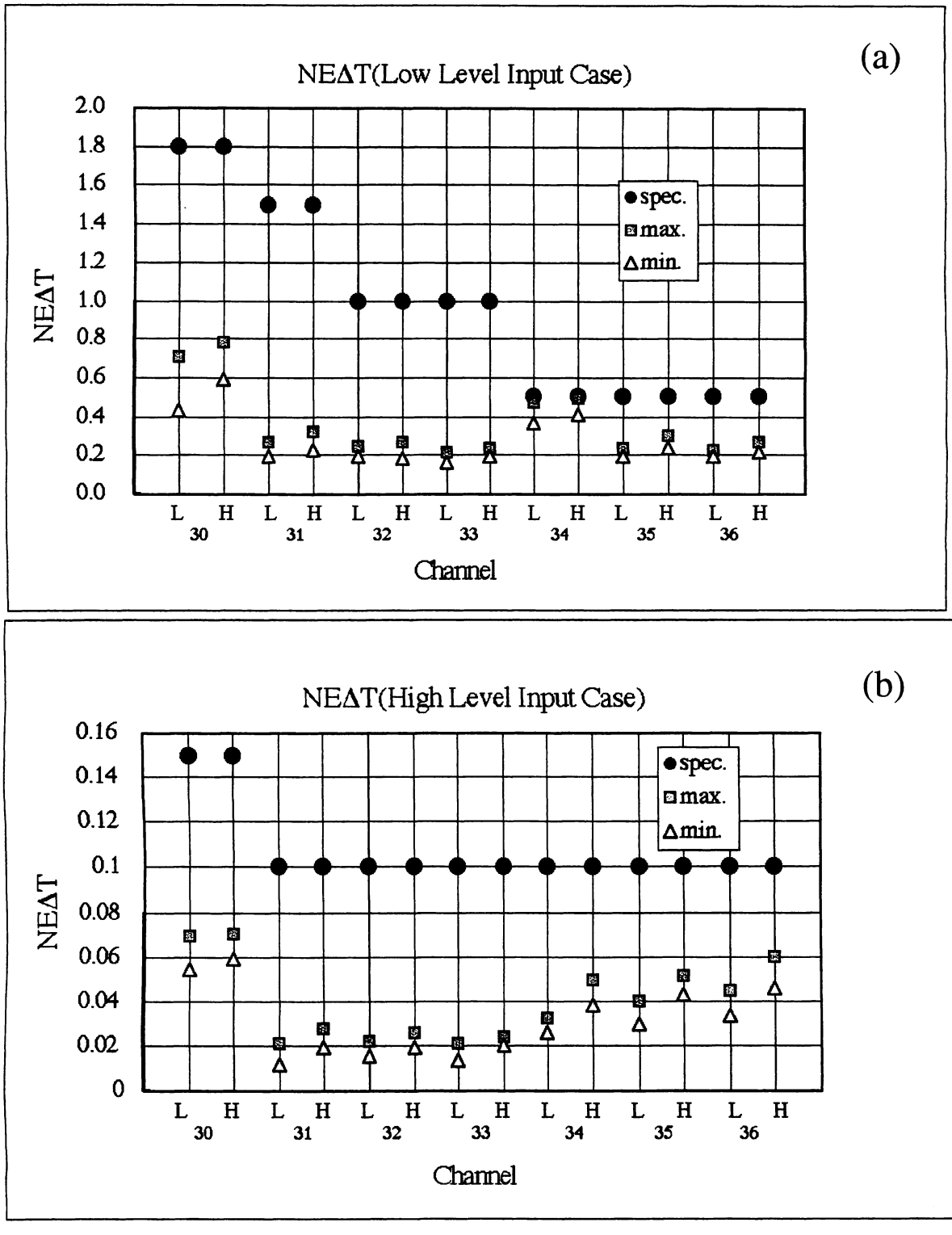

Figure 2 NEDT of the GLI channels(Ch. 30 - Ch. 36). Low level input case (a) and high level input case(b).

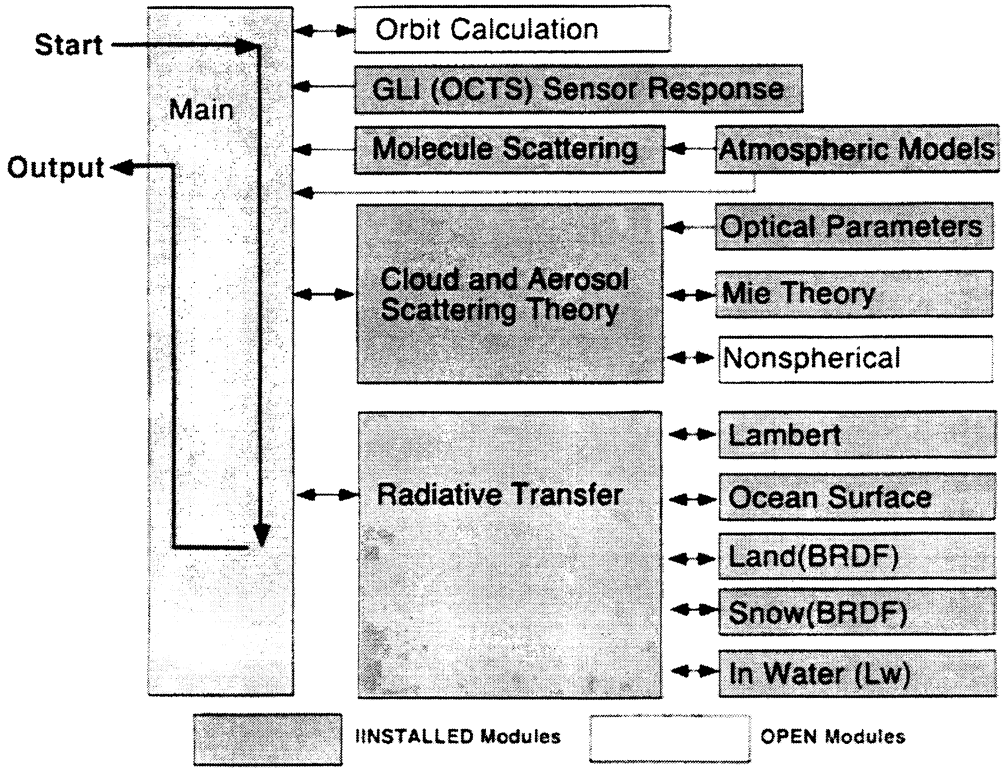

Figure 3 Current structure of the GSS

are two field of view angles of the radiometer, i. e. 1km and 250m at sub-satellite point, depending on channels as indicated in Table 1. Six 250m channels (ch. 20-23, 28, 29) are spectrally similar to LANDSAT/ TM. The globe will be covered by every 4 days with a swath width of about –43 (1600 km).

Construction of the PFM (Proto Flight Model) has been completed by Fujitsu Co. Ltd. in May 1999. Comprehensive testing of the PFM has have revealed the satisfactory performance of the GLI as a remote sensor. Figure 1 and 2 show the S/N ratio and NEDT of the GLI channels. The figures show that the PFM values are equal or larger than the specifications for most of the channels.

3. GLI SIMULATOR AND SIMULATED DATA

The GLI signal simulator (GSS) has been developed as a community tool for development of the algorithms. Figure 3 shows the structure of the GSS, that can simulate the GLI-observed radiances in 36 channels for the model earth-atmosphere system. Vegetation BRDF model[3], snow surface BRDF model[4], and in-water model[5] which calculates normalized upwelling water leaving radiance are implemented in the GSS with model atmospheres with clouds and aerosols. The radiative transfer in the model earth-atmosphere system is accurately calculated by the *R-Star* radiative transfer code. Generated synthetic data sets (GSD) are further used for testing the inversion algorithms and/or end-to-end test of the analysis system. Figure 4 shows an example of the GSD for all the 36 channel radiance imageries. Input geophysical parameter in this case were, AVHRR-derived cloud optical thicknesses and effective particle radii, and cloud top temperatures over the ocean surface.

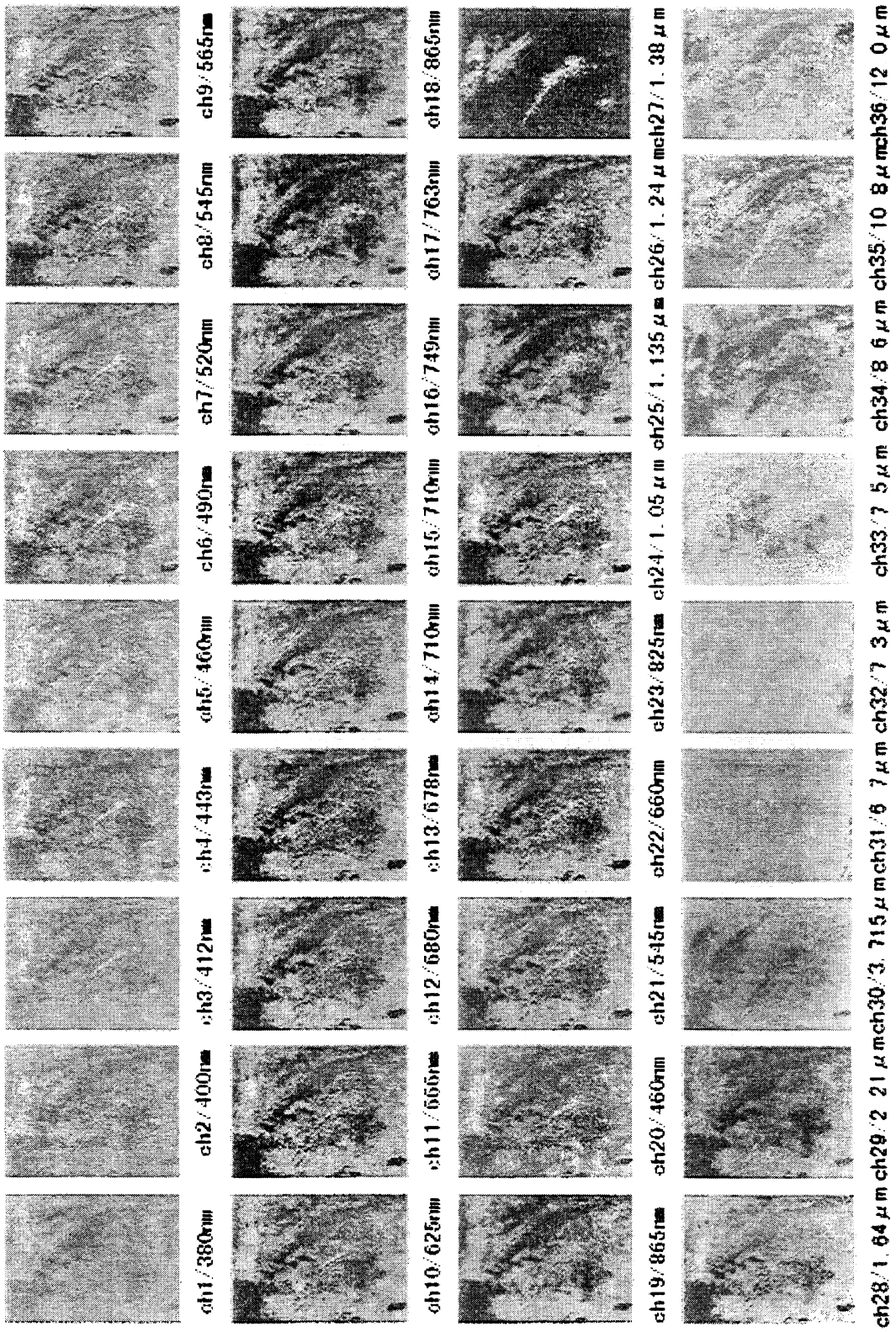

Figure 4. An example of the GLI synthetic data sets (GSD) for 36 channel imagery.

Table 2 The level-2 standard products planned for atmosphere, ocean, land and cryosphere.

Atmosphere	Aerosol	Aerosol Angstrom Exponent (ARAE) Aerosol Optical Thickness (AROP)
	Cloud	Cloud Flag (CLFLG_p) Cloud Optical Thickness (CLOP_p) Cloud Effective Particle Radius (CLER) Cloud Optical Thickness (CLOP) Cloud Top Height (CLHT) Cloud Top Temperature (CLTT) Cloud Liquid Water Path (CLWP) Cloud Type (CLTY) Cloud Fraction (CLFR)
Ocean	Atmospheric Correction (NL_FR) (NL_LR)	Normalized water-leaving radiance (NWLR) Quality Flag (QF_OC)
	In-water (CS_FR) (CS_LR)	Chlorophyll-a (CHLA) Colored Dissolved Organic Matter (CDOM) Attenuation Coeff. at 490nm (K490) Suspended Solid Weight (SS) Quality Flag (QF_OC)
	SST (ST_FR) (ST_LR)	Bulk Sea Surface Temperature (SST_b) Quality Flag (QF_ST)
Land	Atmospheric Correction	Atmospheric Correction (ACLC)
	Precise Geolocation	Precise Geolocation (PGCP)
	Vegetation	Vegetation Index (VGI)
Cryosphere	Snow	Snow Grain Size (SNWG) Snow Impurities (SNWI) Snow/Cloud Flag (SCFG)

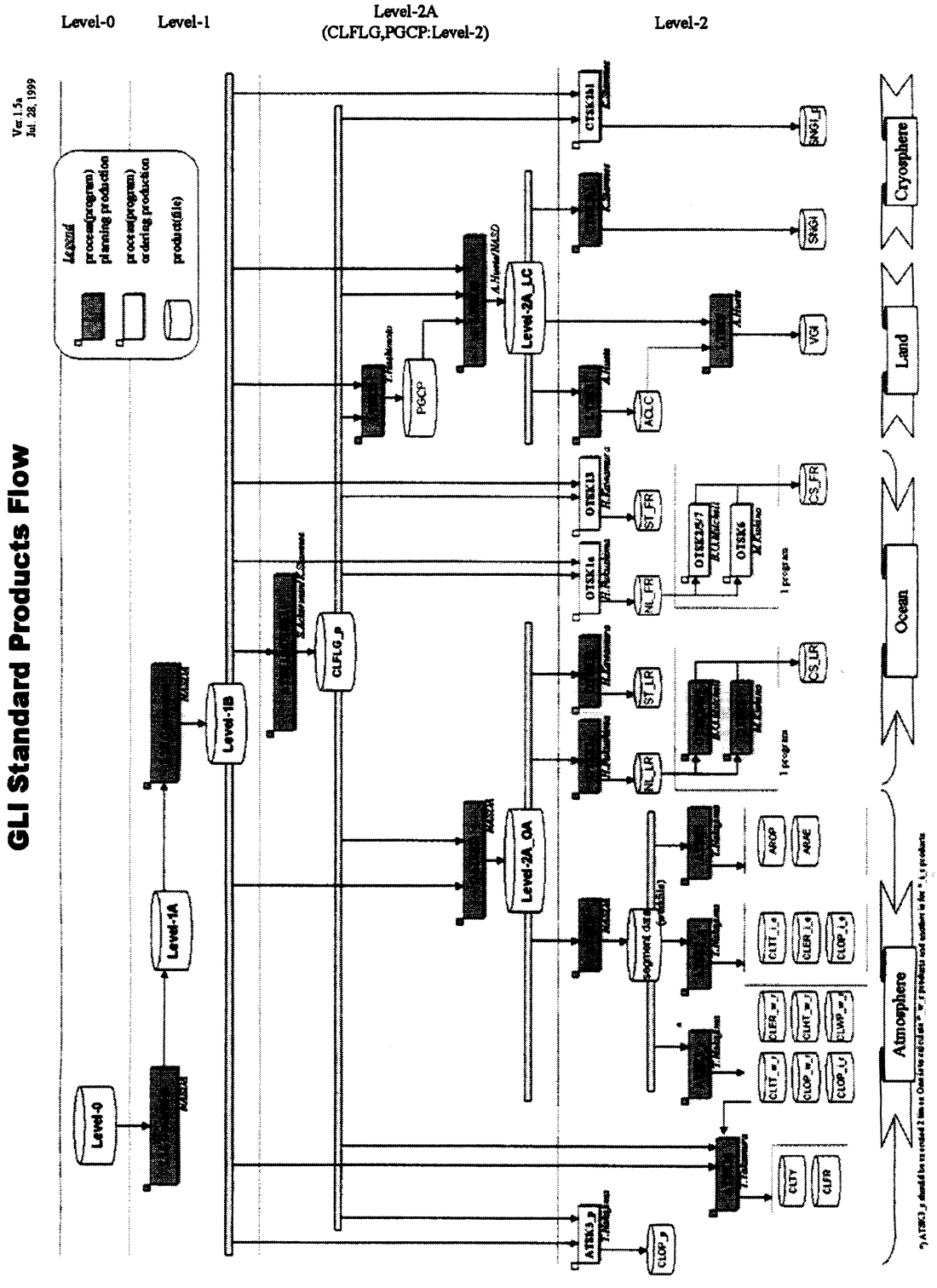

Figure 5 The algorithm flow of the GLI standard products

4. ALGORITHM DEVELOPMENT

The Level-2 standard products are planned as shown in Table 2 for atmosphere, ocean, land and cryosphere. The algorithm flow is also shown in Figure 5.

Cloud flag of Ackerman (1998)[6] will be used with channel 8, 13, 19, 24, 25, 26, 29, 30, 34, 35, and 36. Cloud algorithms, which is an extended version of Nakajima and Nakajima (1995)[7] is further applied for water and ice cloudy pixels. It is found that a rigorous nonspherical scattering model is needed for analyzing visible and 3.7 micron channels (ch. 13 and 30) simultaneously. Clear pixels in channel 13 and 19 will be analyzed by the algorithm of Higurashi and Nakajima (1999)[8] for obtaining the Ångström parameters of aerosols. Water surface leaving radiances will be retrieved by the algorithm of Fukushima et al. (1998)[9]

5. CONCLUSION

We have discussed the current status of the GLI project for hardware and software development. The performance of the PFM is found to be satisfactory as compared with the specifications originally planned. A GLI simulator and simulated data sets are developed as a tool for the algorithm development. It is found an example of the GSD show ample information content of the GLI imagery. The algorithm flow is determined to produce the standard Level-2 products as shown in Table 2.

6. REFERENCES

1. T. Nakajima, Y. Awaya, M. Kishino, T. Ohishi, G. Saitou, A. Uchiyama, T. Y. Nakajima, M. Nakajima, and T. Uesugi, "The current status of the ADEOS-II/GLI mission.," *Advanced and Next-Generation Satellites II*, eds. H. Fujisada, G. Calamai, M. N. Sweeting, SPIE 2957, 183-190, 1997.
2. Nakajima, T. Y., T. Nakajima, M. Nakajima, H. Fukushima, M. Kuji, A. Uchiyama, and M. Kishino, "Optimization of the Advanced Earth Observing Satellite II Global Imager Channels by use of radiative transfer calculations." *Appl. Opt.*, **37**, 3149-3163, 1998.
3. Engelsen, O., B. Pinty, M. M. Verstraete, and J. V. Martonchik, "Parametric bidirectional reflectance factor models: Evaluation, improvement and applications," Office for official publications of the European Communities, 1996.
4. Te. Aoki, Ta. Aoki, M. Fukabori and A. Uchiyama, "Numerical simulation of the atmospheric effect on snow albedo with a multiple scattering radiative transfer model for the atmosphere-snow system," *J. Meteor. Soc. Japan*, **77**, 595-614,1999.
5. A. Tanaka, T. Oishi, M, Kishino, D.Roland, ".Application of the neural network to OCTS data," Proc. of *OCEAN OPTICS XIV*, Hawaii, 1998
6. S. A. Ackerman, K. I. Strabala, W. P. Menzel, R. A. Frey, C. C. Moeller and L. E. Gumley, "Discriminating Clear-sky from Clouds with MODI," S *J. Geo. Res.*, **103** , D24, p. 32,141, 1998
7. T. Y. Nakajima and T. Nakajima, "Wide-area determination of cloud microphysical properties from NOAA AVHRR measurements for FIRE and ASTEX regions," *J. Atmos. Sci.*, **52**, 4043-4059, 1995.
8. Higurashi, A., and T. Nakajima, "Development of a Two Channel Aerosol Retrieval Algorithm on Global Scale Using NOAA / AVHRR." *J. Atmos. Sci.*, 56, 924-941, 1999.
9. Fukushima, H.,A. Higurashi, Y. Mitomi, T. Nakajima, T. Noguchi, T. Tanaka, M. Toratani (1998), Correction of Atmospheric effect on ADEOS/OCTS ocean color data: Algorithm description and evaluation of its performance, *J. Oceanogr.*, **54**, 417-430, 1998